

In vivo experiments

For tumorigenicity assays, syngeneic C57/BL6N mice were subcutaneously challenged with 2.0×10^5 LLC, LLC/SeV/GFP, or LLC/SeV/GM cells with or without imiquimod (R-837; 50 $\mu\text{g}/\text{mouse}$; Invivogen) or lipopolysaccharide (LPS; 5 $\mu\text{g}/\text{mouse}$; Sigma-Aldrich) resuspended in 100- μL Hanks' Balanced Salt Solution (HBSS; Life Technologies) in the right or left flank. To dissect the role of type I IFN and pDCs in the tumorigenicity assays, IFNAR^{-/-} or pDC-depleted mice were subcutaneously challenged with 2.0×10^5 LLC/SeV/GM cells in the right flank. For therapeutic tumor vaccination assays, LLC/SeV/GFP, LLC/SeV/GM, and CT26/SeV/GM cells were irradiated at 50 Gy and were designated as irLLC/SeV/GFP, irLLC/SeV/GM, and irCT26/SeV/GM cells, respectively. On days 2 and 9 after tumor challenge with parental LLC or CT26 cells, C57/BL6N or BALB/cN mice were subcutaneously vaccinated with the indicated tumor vaccine cells in the opposite flank. Tumor volume was measured every 2 to 4 days and calculated with the following formula: $0.4 \times (\text{largest diameter}) \times (\text{smallest diameter})^2$.

ELISA assay

In vitro expression levels of mouse GM-CSF produced from LLC, LLC/SeV/GFP, or LLC/SeV/GM cells at the MOI and time points were measured using mouse GM-CSF enzyme-linked immunosorbent assay (ELISA) kits (R&D Systems).

Flow cytometric analysis

TDLNs, spleen, and tumor vaccine sites (TVS) harvested from the indicated groups of mice ($n = 3-5$) were homogenized and filtered through a 100- μm cell strainer (BD Biosciences). For splenocyte preparation, smashed spleens were treated with ammonium chloride to lyse red blood. For T-cell detection in mixed lymphocyte reaction (MLR) assays, cells were stained with anti-CD4 (RM4.5)–PE (eBioscience), anti-CD3e–APC (145-2C11), and anti-CD8a–PerCP (53-6.7; BioLegend). For phenotypic analyses of DCs in TDLNs, cells were stained with an anti-mouse CD11c Ab [anti-CD11c–APC (N418; BioLegend) in combination with anti-mouse Abs, including anti-B220–PE (RA3-6B2), anti-CD317 (PDCA-1, BST2)–PE (eBio129c; all eBioscience), anti-CD80–PE (16-10A1), anti-CD8a–PerCP, anti-CD86–FITC (GL-1), or anti-CD11b–FITC (M1/70; all BioLegend). For phenotypic analyses of pDCs in TDLNs, cells were stained with either anti-CD317 (PDCA-1, BST2)–PE, anti-PDCA-1–APC (JF05-1C2.4.1; Miltenyi Biotec), or anti-CD11c–PerCPCy5.5 (N418; eBioscience) in combination with anti-mouse Abs, including anti-CD86–FITC, anti-CD9–FITC (MZ3; BioLegend), and anti-Siglec-H–FITC

(551.3D3; Miltenyi Biotec). For regulatory T-cell (Treg) detection in TDLNs, cells were permeabilized with Cytofix/Cytoperm kit (BD Biosciences), washed with BD Perm/Wash buffer (BD Biosciences), and stained with anti-CD4, anti-CD25–FITC (PC61.5), and anti-FoxP3–APC (FJK-16s; all eBioscience). Cells were incubated with Abs and analyzed with BD FACSCalibur flow cytometer, CellQuest software (BD Biosciences), and FlowJo software (TreeStar).

Allogeneic MLR assays

To prepare CD11c⁺ DCs as stimulators, on day 2 of the tumorigenicity assay, CD11c⁺ DCs were purified from TDLNs in mice treated with LLC, LLC/SeV/GFP, or LLC/SeV/GM cells using CD11c MicroBeads (Miltenyi Biotec). To prepare the pDC subset as stimulators, total bone marrow cells harvested from naïve C57/BL6N mice were cultured in RPMI-1640 supplemented with 50 ng/mL murine Fms-related tyrosine kinase 3 ligand (Flt3L; PeproTech) for 8 days and Siglec-H–positive cells (pDCs) were purified using anti-Siglec-H–FITC Ab and anti-FITC MicroBeads (Miltenyi Biotec). Sorted pDCs were then incubated overnight with or without 2.5 $\mu\text{g}/\text{mL}$ of imiquimod or 10 ng/mL of murine recombinant GM-CSF (PeproTech). To prepare allogeneic T cells as responders, T cells were sorted from splenocytes harvested from naïve BALB/cN mice using a Pan T-cell isolation kit II (Miltenyi Biotec). A total of 5.0×10^4 responder T cells labeled with 1.0 $\mu\text{mol}/\text{L}$ CFSE [5(6)-carboxyfluorescein diacetate N-succinimidylester; Sigma-Aldrich] were cocultured with an equal number of 30 Gy–irradiated CD11c⁺ DCs. A total of 2.0×10^5 T cells labeled with 2.5 $\mu\text{mol}/\text{L}$ of CFSE were cocultured with 4.0×10^4 of pDCs for 5 days. The proliferation rate of the gated CD3⁺ T-cell fraction was visualized by CFSE dilution.

Detection of DCs that engulfed TAAs

LLC, LLC/SeV/GFP, and LLC/SeV/GM cells were labeled with the PKH26 Red Fluorescent Cell Linker Mini Kit (Sigma-Aldrich), respectively, according to the manufacturer's instruction. On day 2 after they were subcutaneously injected into the right flanks of mice, axillary lymph nodes in both TDLNs and CLNs were harvested, incubated with anti-CD86–FITC and anti-CD11c–APC Abs, and subjected to flow cytometric analysis.

cDNA microarray

Dead cells were excluded from CD86⁺CD11c⁺ DCs using 7-AAD viability dye (Beckman Coulter), which were sorted by

Figure 3. Transcriptome analysis suggested the involvement of type I IFN–related pathways in GM-DCs during GM-CSF–induced antitumor immunity. A, total RNA was isolated from CD86⁺ DCs in TDLNs from mice inoculated with LLC, LLC/SeV/GFP, or LLC/SeV/GM cells 2 days after the tumor challenge and subjected to cDNA microarray. The top 10 canonical pathways significantly upregulated in GM-DCs, in comparison with those in GFP-DCs, by which a right-tailed Fisher exact test was calculated using the entire dataset. B, IPA was performed using the type I IFN pathway–related genes from the original commonly regulated probes differentially expressed between GFP-DCs and GM-DCs. Differentially expressed genes are indicated in red and green, representing up- and downregulation induced by GM-CSF activation, respectively. A high degree of gene regulation is indicated by bold-colored genes. Direct or indirect associations with the differentially expressed genes indicated by no color were not found to be significantly different in this assessment. Positive regulatory interactions are depicted by solid arrows (direct interactions) or dashed arrows (indirect interactions). C, heatmap based on type I IFN pathway–related genes that were differentially expressed in CD86⁺ DCs in TDLNs from indicated mouse groups. D, cell numbers of DC subsets (pDC, CD8⁺ cDCs, and CD11b⁺ cDC) in TDLNs at days 2 (top) and 4 (bottom) after the respective tumor challenge were comparatively quantified (*, $P < 0.05$; **, $P < 0.01$). E and F, representative tumor growth curves observed in IFNAR^{-/-} (E) or pDC-depleted (F) mice (**, $P < 0.01$).

FACSAria (BD Biosciences) from TDLNs of mice on day 2 during the tumorigenicity assay. Cells were transferred to RNA later (Life Technologies) to stabilize and protect intact cellular RNA. RNA isolation was performed according to the TRIzol Reagent technical manual (Life Technologies). Total RNA (50 ng) was amplified and labeled using the Agilent Low-Input QuickAmp Labeling Kit, one color (Agilent Technologies). Labeled cRNA was hybridized to Agilent Whole Mouse Genome Oligo DNA microarray (4 × 44 K) v2 (Agilent Technologies). All gene transcription products were hybridized to microarray slides and were scanned by an Agilent scanner. Relative hybridization intensities and background hybridization values were calculated using the Agilent Feature Extraction Software (v9.5.1.1; Agilent Technologies). The raw signal intensities of two samples were \log_2 -transformed and normalized by a quantile algorithm with the "preprocessCore" library package on Bioconductor software. We used Z-scores to compare significant changes in gene expression in each of the three groups (DCs from mice treated with LLC, LLC/SeV/GFP, and LLC/SeV/GM cells). Lists of genes with statistically significant expression in GM-DCs in comparison with GFP-DCs were submitted to Ingenuity Pathway Analysis (IPA; Ingenuity Systems) and analyzed for overrepresented general functions and the resulting networks. Microarray data were deposited in Gene Expression Omnibus (GEO; <http://www.ncbi.nlm.nih.gov/geo/>; accession number GSE43169).

In vivo depletion experiments

To deplete pDCs, mice were injected intraperitoneally with 100 μ g of anti-PDCA-1 mAb (JF05-1C2.4.1; Miltenyi Biotec) or control Ab (rat IgG; Jackson ImmunoResearch), as previously described (7). Effective depletion of PDCA-1⁺ cells was confirmed by flow cytometric analysis (Supplementary Fig. S1). CD4⁺ T or CD8⁺ T cells were depleted by using GK1.5 or 2.43 mAbs, as previously described (8). Briefly, mice received intraperitoneal injections of anti-mouse GK1.5 mAb, anti-mouse 2.43 mAb (50 μ g/mouse), or control Ab 6, 4, and 2 days before tumor challenge, and once every 3 days thereafter. Effective depletion of CD4⁺ and CD8⁺ T cells was confirmed by flow cytometric analysis (data not shown).

Results

Production of GM-CSF from LLC and B16F10 cells remarkably impaired the tumorigenicity

To test the possibility that substantial secretion of GM-CSF from syngeneic mouse cancer cells facilitates the development of antitumor immune responses, we used recombinant non-transmissible Sendai virus vectors expressing GM-CSF (SeV/GM) at various MOI. Abundant GM-CSF production from the infected LLC (LLC/SeV/GM) cells was observed and was MOI dependent (Fig. 1A). The proliferation rate of LLC cells was not affected by transduction with SeV/GM, as previously described (6). We next performed tumorigenicity assays in which each LLC and LLC/SeV/GM cells (MOI = 1, 10, and 100) were subcutaneously injected into the left flank of syngeneic mice. All mice treated with LLC/SeV/GM cells exhibited significant suppression of the tumor outgrowth in an MOI-dependent manner (Fig. 1B). We thus determined MOI = 100 for gene

transduction as an optimized infection dose. Notably, mice treated with LLC/SeV/GM cells showed significantly suppressed tumor growth and prolonged survival of mice, compared with control groups ($P < 0.001$; Fig. 1C). Similar suppression of tumor growth and prolongation of mouse survival were observed when SeV/GM-infected B16F10 melanoma cells were injected to C57BL/6N mice (Fig. 1D).

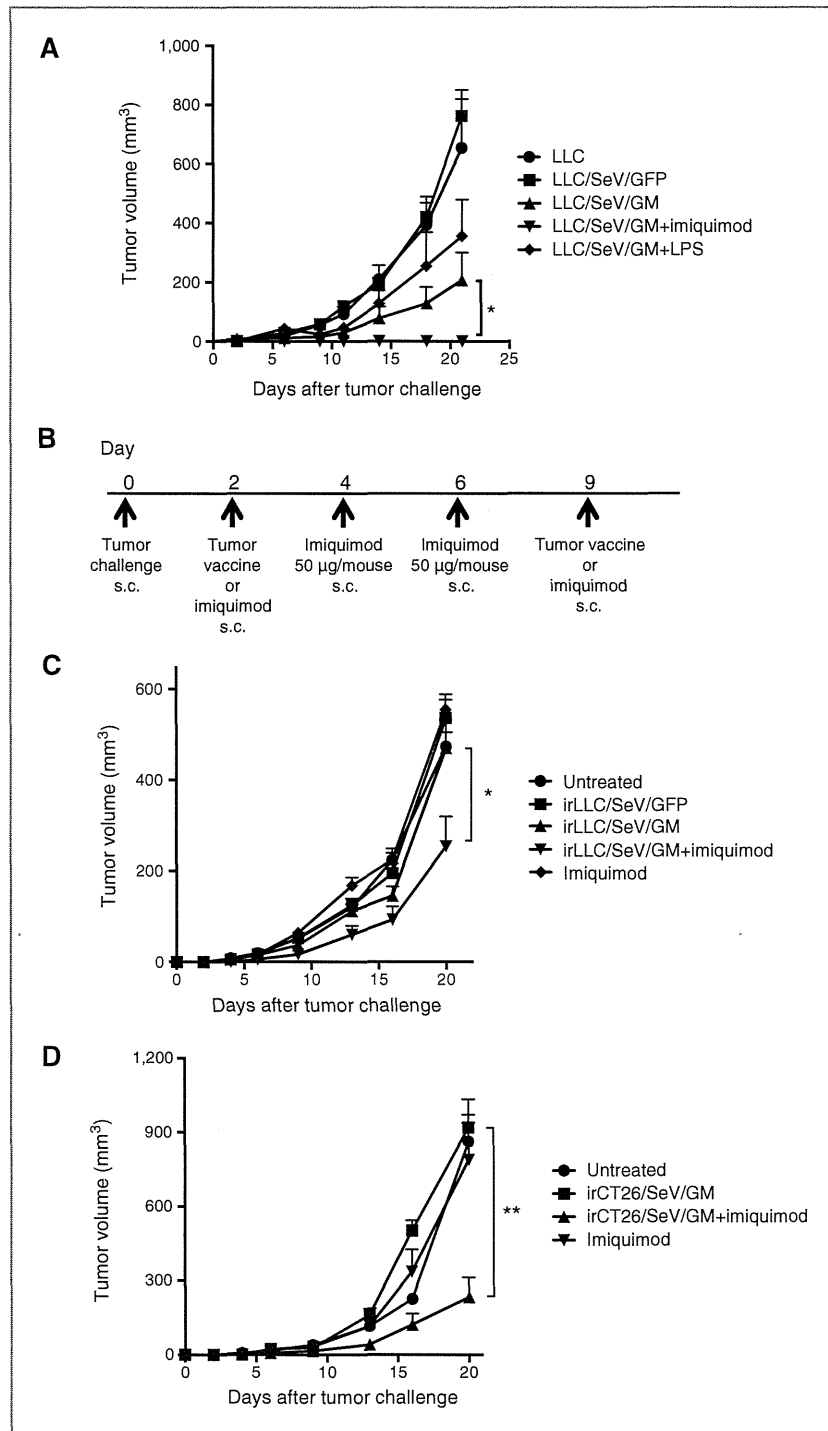
Increased ability of GM-CSF-sensitized DCs to stimulate T-cell proliferation, accelerate their maturation, and deliver phagocytosed TAAs in TDLNs

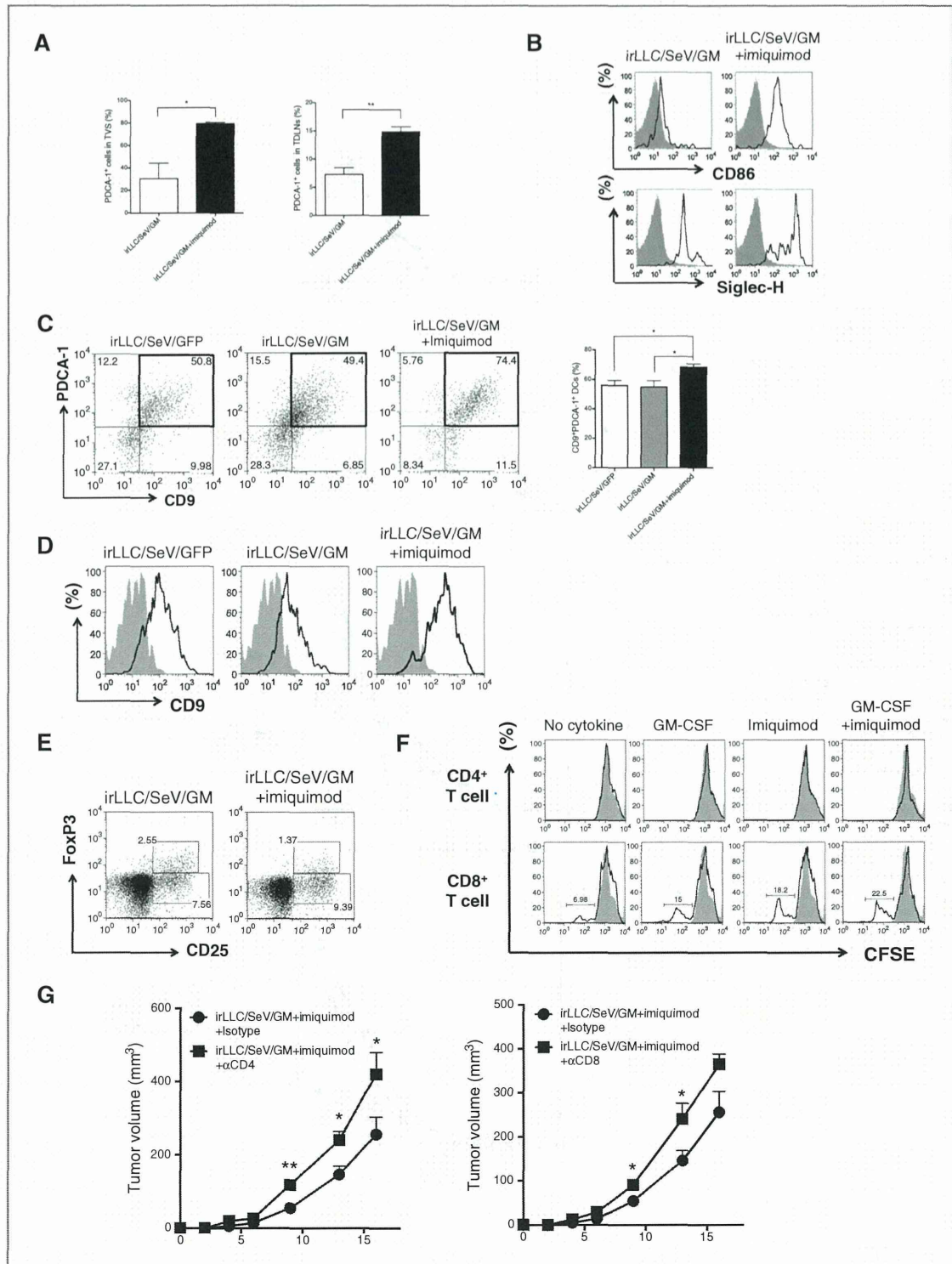
To determine a putative phase when GM-CSF-sensitized DCs from TDLNs of mice treated with LLC/SeV/GM cells (GM-DCs) effectively prime naïve T cells, we performed allogeneic MLR assays. GM-DCs exhibited a significantly marked response on day 2 compared with DCs from mice treated with LLC/SeV/GFP cells (GFP-DCs), and stimulated the proliferation of allogeneic CD3⁺CD4⁺ T and CD3⁺CD8⁺ T cells (Fig. 2A). Furthermore, GM-DCs harvested on day 2 elicited higher expression levels of costimulatory maturation markers CD80 and CD86 than those from control mice (Fig. 2B), suggesting that day 2 could be the putative phase to mount optimum immunologic responses by GM-DCs. To explore the migratory capacity of GM-DCs that phagocytosed TAAs at the tumor injection site, we inoculated PKH26-labeled LLC, LLC/SeV/GFP, or LLC/SeV/GM cells into the right flank of mice, and evaluated PKH26⁺ DC numbers in both TDLNs and contralateral LNs (CLN). The frequencies of PKH26⁺ DCs in TDLNs, but not CLNs, harvested from mice treated with LLC/SeV/GM cells were significantly increased, indicating that GM-CSF production potentiated the migration of PKH26-labeled LLC cells (TAA)-phagocytosed DCs from the tumor injection site into TDLNs ($P < 0.05$; Fig. 2C). PKH26⁺ GM-DCs derived from TDLNs, but not from CLNs, showed significantly higher CD86 expression than controls ($P < 0.001$; Fig. 2D).

cDNA microarray analysis revealed the involvement of type I IFN-related pathways in GM-CSF-induced antitumor immunity

On the basis of the aforementioned results, we determined day 2 to be an adequate time point for the peak in T-cell priming by TAA-phagocytosed CD86⁺ DCs. To address the important factor of DC/T-cell priming, we isolated CD86⁺ DCs from mice treated with LLC/SeV/GM cells and control groups, and compared the comprehensive gene expression patterns of isolated CD86⁺ DCs in TDLNs. After normalization of microarray data and statistical analysis, 1,318 genes were found to be differentially expressed between GM-DCs and GFP-DCs with statistical significance (upregulated genes; Z-score ≥ 2 and ratio > 1.5 , downregulated genes; Z-score ≤ -2 and ratio < 0.66 ; data not shown). A list of the genes significantly upregulated in the top 10 canonical pathways in CD86⁺ GM-DCs in comparison with CD86⁺ GFP-DCs is shown in Table 1. As expected, these genes composed immunologic response-related pathways (Fig. 3A). Among the activated pathways triggered by GM-CSF, we focused on the following representative molecules: IRF7, OAS3 (2'-5'-oligoadenylate synthetase 3), and TLR7, which constitute the type I IFN (IFN- α /IFN- β)-associated pathways (Fig. 3B and C;

Figure 4. Combined imiquimod and irLLC/SeV/GM cells exert significant therapeutic antitumor effects compared with irLLC/SeV/GM cells alone. A, a total of 2.0×10^5 LLC and LLC/SeV/GM cells with or without LPS or imiquimod were subcutaneously inoculated into the right flanks of C57/BL6N mice. Bar graphs, mean \pm SEM of tumor volumes. Combined data from two independent experiments with similar results are shown (*, $P < 0.05$). B, schematic diagram of the experimental protocol of therapeutic GM-CSF-based tumor vaccination. Briefly, 2.0×10^5 LLC cells or 3.0×10^5 CT26 cells were inoculated subcutaneously to C57/BL6N or BALB/cN mice. LLC-bearing mice were divided into the following groups: untreated, imiquimod alone, irLLC/SeV/GFP, irLLC/SeV/GM, or irLLC/SeV/GM cells plus imiquimod. CT26-bearing mice were divided into the following groups: untreated, imiquimod alone, irCT26/SeV/GM or irCT26/SeV/GM cells plus imiquimod. On days 2 and 9, mice were inoculated subcutaneously with the indicated vaccine cells. For imiquimod administration, mice were subcutaneously inoculated with imiquimod on days 2, 4, 6, and 9. Represented are tumor growth curves observed in either LLC- (C) or CT26-bearing (D) mice (*, $P < 0.05$; **, $P < 0.01$).





refs. 5, 9). Microarray results for the expression levels of *Irf7* and *Oas3* were validated by performing qRT-PCR (Supplementary Fig. S2). As pDCs provoke initial defensive antiviral responses by type I IFN production and are the main producers of type I IFNs (10), we speculated that pDCs could be positively involved in the induction of effective GM-CSF–sensitized DC/T-cell priming (11). Indeed, the numbers of pDCs, CD11b⁺ cDCs, and CD8⁺ cDCs subsets from total GM-DCs from TDLNs harvested on days 2 and 4 were greater than the equivalent subsets from total GFP-DCs (Fig. 3D). Furthermore, the results of *in vivo* experiments using IFN α receptor knockout (IFNAR^{-/-}) mice demonstrated that IFNAR^{-/-} mice inoculated with LLC/SeV/GM cells significantly abrogated the impairment of tumorigenicity seen in the corresponding wild-type (WT) mice (Fig. 3E). Importantly, similar results were also obtained when pDC-depleted mice were used (Fig. 3F). These results collectively demonstrate the positive role of type I IFN–producing pDCs in the induction of GM-CSF–mediated antitumor immunity.

Combination of TLR7 ligand and GM-CSF–secreting LLC cells enhanced the induction of antitumor immunity in both tumorigenicity and therapeutic vaccination models

TLR7-dependent type I IFN pathways are activated by binding with their corresponding ligand, imiquimod (12). To examine the impact of the TLR7-mediated activation of type I IFN–related pathways primarily in pDCs on GM-CSF–induced antitumor immunity, we performed a gain-of-function assay by evaluating the tumorigenicity of LLC/SeV/GM cells with or without imiquimod or TLR4 ligand, LPS, as an irrelevant control. Mice treated with LLC/SeV/GM cells combined with imiquimod showed significantly suppressed tumor development accompanied with complete tumor regression ($P < 0.05$). Conversely, treatment with LLC/SeV/GM cells combined with LPS attenuated the GM-CSF–induced antitumor effects (Fig. 4A), and these mice exhibited no significant changes in body weight (Supplementary Fig. S3). We next attempted to translate these findings into a tumor vaccination therapy by adding imiquimod to the subcutaneous administration of irradiated LLC/SeV/GM (irLLC/SeV/GM) cells to investigate the synergistic effect. Notably, mice treated with combined imiquimod and irLLC/SeV/GM cells elicited a significantly marked suppression of tumor growth of preestablished LLC cells, whereas control mice treated with irLLC/SeV/GM cells or imiquimod alone manifested negligible antitumor effects ($P < 0.05$; Fig. 4B and C). Similarly, mice vaccinated

with irradiated GM-CSF gene-transduced (MOI = 100) CT26 colon cancer cells in combination with imiquimod showed significantly suppressed tumor development ($P < 0.01$; Fig. 4D).

Admixed use of TLR7 ligand in combination with GVAX therapy induced pDC activation leading to generation of T-cell–mediated antitumor immunity

To elucidate the effect of imiquimod on GM-CSF–induced initial immune responses, we performed phenotypic immunanalyses. Six hours after the first tumor vaccination, mice treated with irLLC/SeV/GM cells plus imiquimod showed a significantly higher frequency and number of cells expressing PDCA-1, a pDC-specific marker, than control mice in both TVSs and TDLNs (Fig. 5A and Supplementary Fig. S4). Furthermore, pDCs (CD11c⁺PDCA-1⁺ cells) derived from mice treated with irLLC/SeV/GM cells plus imiquimod expressed increased levels of CD86 and sialic acid binding Ig-like lectin (Siglec)-H, a functional pDC-specific receptor (Fig. 5B; ref. 13), accompanied with significantly higher levels of serum IFN α (Supplementary Fig. S5). Because CD9⁺ pDCs stimulated with TLR agonists induced higher amounts of IFN α and provoked protective T-cell–mediated antitumor immunity (14), we compared CD9 expression levels on pDC subsets. Mice treated with irLLC/SeV/GM cells plus imiquimod had significantly increased frequency and mean fluorescence intensity (MFI) of CD9⁺PDCA1⁺CD11c⁺ pDCs in TDLNs (Fig. 5C and D). However, the frequency of CD4⁺CD25⁺FoxP3⁺ Tregs was decreased in TDLNs from mice treated with irLLC/SeV/GM cells and imiquimod, whereas the frequency of CD4⁺CD25⁺FoxP3⁻ T cells was increased in mice treated with combined therapy (Fig. 5E). To investigate the effect of imiquimod and GM-CSF on the T-cell proliferation capacity of pDCs, we performed an allogeneic MLR assay. pDCs stimulated with GM-CSF and imiquimod elicited the most pronounced proliferative activity of CD8⁺ T cells, but not CD4⁺ T cells, when compared with controls (Fig. 5F). Moreover, the synergistic therapeutic efficacy of irLLC/SeV/GM cells and imiquimod was significantly inhibited when the corresponding mice were depleted of CD4⁺ or CD8⁺ T cells (Fig. 5G).

Discussion

This study demonstrates that SeV/dF-mediated exogenous expression of GM-CSF caused poor growth of cancer cells in

Figure 5. Mice vaccinated with combined irLLC/SeV/GM cells and imiquimod augmented the recruitment of activated pDCs in TDLNs. A, 6 hours after the first tumor vaccination, infiltrating lymphocytes in TVSs or TDLNs were harvested from indicated mouse groups. Bar graphs, mean \pm SEM of frequency of PDCA-1⁺ cells gated on FSC/SSC profiles. B, histograms represent expression levels of Siglec-H or CD86 expression on CD11c⁺PDCA-1⁺ cells (pDCs) in TDLNs from indicated mouse groups (tinted light gray, isotype control; bold line, anti-CD86 or anti-Siglec-H Ab. C, on day 12, TDLNs were harvested from mice treated with irLLC/SeV/GFP, irLLC/SeV/GM, or irLLC/SeV/GM cells plus imiquimod ($n = 3$). Representative dot plots depict CD9 and PDCA-1 expression gated on CD11c⁺ cells in TDLNs (left). Bar graphs, mean \pm SEM of frequency of CD9⁺PDCA-1⁺ cells on DCs (*, $P < 0.05$; right). D, histograms depict MFI representing CD9 expression levels on PDCA-1⁺CD11c⁺ subpopulations in TDLNs (tinted light gray, isotype control; bold line, anti-CD9 Ab). E, representative dot plots illustrate CD25 and FoxP3 expression gated on CD4⁺ T cells in TDLNs from indicated mouse groups. F, CFSE-labeled allogeneic MLR assay. Bone marrow–derived pDCs treated with GM-CSF or imiquimod or in combination with GM-CSF plus imiquimod were mixed with CFSE-labeled T cells. Representative histograms show CFSE expression of allogeneic CD4⁺CD3⁺ or CD8⁺CD3⁺ T cells stimulated by the indicated pDCs. G, tumor growth curves in CD4⁺ T-cell (left)– or CD8⁺ T-cell (right)–depleted mice treated with irLLC/SeV/GM cells plus imiquimod (*, $P < 0.05$; **, $P < 0.01$).

syngeneic mice, concomitant with an early appearance of mature DCs in TDLNs. We used SeV/dF vectors for the gene transduction of vaccine cells because they have relatively higher capacities in terms of gene transduction, induction of antitumor immunity, and safety (6, 15). Expression microarray analyses of the GM-CSF-sensitized CD86⁺ DCs revealed increased expression of the TLR7-IRF7 pathway components, which induce type I IFN production in pDCs (5). Furthermore, the addition of imiquimod was found to be an effective potential approach to improve the antitumor effects of GVAX therapy (Fig. 4).

As LLC cells have been considered as poorly immunogenic in lung cancer (16), it was surprising that tumor challenge with LLC/SeV/GM cells markedly impaired its tumorigenicity with complete tumor disappearance in half of the mice tested (Fig. 1). In addition, prophylactic vaccination with irLLC/SeV/GM cells also significantly inhibited subsequent tumor challenge with LLC cells (Supplementary Fig. S6). However, therapeutic vaccination using irLLC/SeV/GM cells alone failed to exert significant antitumor immunity (Fig. 4C). We, therefore, attempted to potentiate the therapeutic antitumor effects of irLLC/SeV/GM cells through scrutinizing the gene expression signature of GM-CSF-sensitized DCs in TDLNs from mice that strongly rejected the tumor challenge with LLC/SeV/GM cells. We confirmed that GM-CSF facilitated the maturation of DCs into antigen-presenting cells with enhanced ability to prime naïve T cells to proliferate, and to increase expression of CD80, CD86, MHC class I, MHC class II, and CD40 (Fig. 2B and Supplementary Fig. S7), consistent with the previous finding that GM-CSF promotes DCs maturation and differentiation (17). Herein, transcriptome analyses revealed that GM-CSF also modulated signal transduction in pDCs by upregulation of the TLR7-IRF7 pathway related to type I IFN production (Fig. 3), consistent with a previous report that GM-CSF stimulation upregulated TLR7 expression in mouse immune cells (18). Our observation that the pDC subset was markedly increased in GM-DCs from TDLNs was unexpected, as the GM-CSF receptor is mainly expressed on CD34⁺ progenitor cells and myeloid cells (19, 20), and GM-CSF administration preferentially expands CD11b⁺ cDC (21, 22) and inhibits pDC differentiation (23). However, recent studies showing that pDC precursors differentiated to CD11b⁺MHC II^{high} cDCs by GM-CSF stimulation (24), and the identification of GM-CSF as a novel activator of pDCs revealed by systematic analysis of cytokine receptors (25), may explain the increase of GM-CSF-sensitized pDC subsets in TDLNs (Fig. 3D). In the development of active immunotherapeutic strategies, much attention has been focused on CD11b⁺ cDC-based vaccines that have failed to induce sufficient clinical efficacy (26), as pDCs are considered to be involved in the maintenance of antitumor tolerance (27) and to be inversely correlated with prognosis in patients with cancer (28, 29). However, pDC subsets can be pivotal players in TAA-specific antitumor immune responses by functioning as antigen-presenting cells (30) that use distinct MHC class II antigen-presentation molecules (31), leading to the effective priming of naïve

CD4⁺ T cells (32), and cross-present antigens with an efficiency comparable with CD11b⁺ cDCs (33), implicating their potential as promising antigen-presenting cells for cancer immunotherapy. Indeed, imiquimod or CpG, a TLR9 agonist, reverted immunotolerant pDCs to antitumor pDCs (34), resulting in clinical antitumor effects (35, 36). Importantly, results of our *in vivo* experiments using pDC depletion and/or IFNAR^{-/-} mice demonstrated the positive impact of the pDC subset and/or type I IFN signaling on the effective generation of GM-CSF-induced antitumor immunity (Fig. 3E and F). Thus, there may be a functional dichotomy in pDC biology between immune tolerance and antitumor phenotype, where their redirection is dependent on the tumor microenvironment.

Imiquimod, a TLR7 ligand, could be regarded as the most effective adjuvant among all approved immunomodulators based on the following: (i) topical imiquimod is currently FDA approved with a good safety profile; (ii) it potently activates antigen-presenting cells to release type I IFNs and Th1-skewing cytokines; and (iii) imiquimod treatment leads to CCL2-dependent recruitment of pDCs and their transformation into killer DCs (37). The underlying mechanism of substantial antitumor efficacy by the combined vaccination may be due to generation of functionally mature pDCs in TVSS and TDLNs (Fig. 5A and Supplementary Fig. S4). IFN α , mainly produced from pDCs upon exposure to viruses via TLR7 or TLR9 (38), acts directly on memory T cells, which potentiate the antigen presentation and cross-priming capacities of CD11b⁺ cDCs (39, 40). We detected CD9⁺ pDCs, which produce abundant IFN α (14), in TDLNs from mice injected with irLLC/SeV/GM cells (Fig. 5C and D). Furthermore, GM-CSF-sensitized pDCs expressed higher CD86 and Siglec-H (Fig. 5B), a regulator of pDC differentiation and CD8⁺ T-cell responses (13, 41). Moreover, pDCs activated with GM-CSF plus imiquimod further enhanced the proliferation of CD8⁺ T cells (Fig. 5F), indicating that GM-CSF-activated pDCs with or without imiquimod could serve as functional antigen-presenting cells to prime the potent generation of TAA-specific adaptive immunity. ELISPOT assay demonstrated that the number of IFN γ -producing splenocytes from mice treated with irLLC/SeV/GM cells plus imiquimod was increased compared with control mice (data not shown). Indeed, depletion assays revealed that CD4⁺ and CD8⁺ T cells significantly contributed to the augmentation of the antitumor efficacy by combination GVAX therapy (Fig. 5G), thus reflecting the imiquimod-driven accelerated TAA-specific Th1 responses.

Although other researchers showed that the addition of imiquimod negates the antitumor efficacy of a GM-CSF-based vaccine (42), these conflicting results may stem from the difference in doses and administration schedule. It is noteworthy that the ability of imiquimod to potentiate the antitumor effect of GVAX therapy in two different types of cancers and in two different host strains might confirm the generality of our findings (Fig. 4C and D).

In conclusion, we, for the first time, elucidated that the beneficial roles of the pDCs and relevant type I IFN pathway

in GM-CSF-induced antitumor immunity and that the combination use of imiquimod with GVAX therapy produced synergistic antitumor effects, underscoring its potential as a promising approach for the treatment of cancer.

Disclosure of Potential Conflicts of Interest

No potential conflicts of interest were disclosed.

Authors' Contributions

Conception and design: M. Narusawa, H. Inoue, Y. Matsumura, K. Tani
Development of methodology: M. Narusawa, H. Inoue, Y. Matsumura, M. Inoue, M. Hasegawa
Acquisition of data (provided animals, acquired and managed patients, provided facilities, etc.): M. Narusawa, H. Inoue, C. Sakamoto, Y. Matsumura, A. Watanabe, K. Tani
Analysis and interpretation of data (e.g., statistical analysis, biostatistics, computational analysis): M. Narusawa, H. Inoue, Y. Matsumura, T. Inoue, S. Miyamoto
Writing, review, and/or revision of the manuscript: M. Narusawa, H. Inoue, A. Takahashi, Y. Tanaka, K. Takayama, T. Okazaki, Y. Nakanishi

Administrative, technical, or material support (i.e., reporting or organizing data, constructing databases): Y. Matsumura, T. Inoue, Y. Miura, M. Hasegawa, K. Tani
Study supervision: H. Inoue, Y. Matsumura, A. Takahashi, Y. Hijikata, T. Okazaki, K. Tani

Acknowledgments

The authors thank Michiyo Okada, Michiko Ushijima, Yosuke Yokota, and Haruka Nabeta for excellent technical assistance, and Kaori Yasuda and Atsushi Doi for performing the cDNA microarray analysis. The authors also thank Katsuaki Sato for valuable discussion.

Grant Support

This work was supported by JSPS KAKENHI grant number 21790773 and a grant for students through the Kyushu University Foundation research grant program.

The costs of publication of this article were defrayed in part by the payment of page charges. This article must therefore be hereby marked *advertisement* in accordance with 18 U.S.C. Section 1734 solely to indicate this fact.

Received September 5, 2013; revised February 5, 2014; accepted March 3, 2014; published OnlineFirst April 10, 2014.

References

1. Dranoff G, Jaffee E, Lazenby A, Golumbek P, Levitsky H, Brose K, et al. Vaccination with irradiated tumor cells engineered to secrete murine granulocyte-macrophage colony-stimulating factor stimulates potent, specific, and long-lasting anti-tumor immunity. *Proc Natl Acad Sci U S A* 1993;90:3539-43.
2. Tani K, Azuma M, Nakazaki Y, Oyaizu N, Hase H, Ohata J, et al. Phase I study of autologous tumor vaccines transduced with the GM-CSF gene in four patients with stage IV renal cell cancer in Japan: clinical and immunological findings. *Mol Ther* 2004;10:799-816.
3. Longo DL. New therapies for castration-resistant prostate cancer. *N Engl J Med* 2010;363:479-81.
4. Li HO, Zhu YF, Asakawa M, Kuma H, Hirata T, Ueda Y, et al. A cytoplasmic RNA vector derived from nontransmissible Sendai virus with efficient gene transfer and expression. *J Virol* 2000;74:6564-9.
5. Honda K, Yanai H, Negishi H, Asagiri M, Sato M, Mizutani T, et al. IRF-7 is the master regulator of type-I interferon-dependent immune responses. *Nature* 2005;434:772-7.
6. Inoue H, Iga M, Nabeta H, Yokoo T, Suehiro Y, Okano S, et al. Non-transmissible Sendai virus encoding granulocyte macrophage colony-stimulating factor is a novel and potent vector system for producing autologous tumor vaccines. *Cancer Sci* 2008;99:2315-26.
7. Yoneyama H, Matsuno K, Toda E, Nishiwaki T, Matsuo N, Nakano A, et al. Plasmacytoid DCs help lymph node DCs to induce anti-HSV CTLs. *J Exp Med* 2005;202:425-35.
8. Yokota Y, Inoue H, Matsumura Y, Nabeta H, Narusawa M, Watanabe A, et al. Absence of LTB4/BLT1 axis facilitates generation of mouse GM-CSF-induced long-lasting antitumor immunologic memory by enhancing innate and adaptive immune systems. *Blood* 2012;120:3444-54.
9. Sadler AJ, Williams BR. Interferon-inducible antiviral effectors. *Nat Rev Immunol* 2008;8:559-68.
10. Gilliet M, Cao W, Liu YJ. Plasmacytoid dendritic cells: sensing nucleic acids in viral infection and autoimmune diseases. *Nat Rev Immunol* 2008;8:594-606.
11. Colonna M, Trinchieri G, Liu YJ. Plasmacytoid dendritic cells in immunity. *Nat Immunol* 2004;5:1219-26.
12. Akira S, Hemmi H. Recognition of pathogen-associated molecular patterns by TLR family. *Immunol Lett* 2003;85:85-95.
13. Takagi H, Fukaya T, Eizumi K, Sato Y, Sato K, Shibazaki A, et al. Plasmacytoid dendritic cells are crucial for the initiation of inflammation and T cell immunity *in vivo*. *Immunity* 2011;35:958-71.
14. Bjorck P, Leong HX, Engleman EG. Plasmacytoid dendritic cell dichotomy: identification of IFN-alpha producing cells as a phenotypically and functionally distinct subset. *J Immunol* 2011;186:1477-85.
15. Shi L, Chen J, Zhong Q, Li M, Geng P, He J, et al. Inactivated Sendai virus strain Tianjin, a novel genotype of Sendai virus, inhibits growth of murine colon carcinoma through inducing immune responses and apoptosis. *J Transl Med* 2013;11:205.
16. Sumimoto H, Tani K, Nakazaki Y, Tanabe T, Hibino H, Hamada H, et al. GM-CSF and B7-1 (CD80) co-stimulatory signals co-operate in the induction of effective anti-tumor immunity in syngeneic mice. *Int J Cancer* 1997;73:556-61.
17. Wada H, Noguchi Y, Marino MW, Dunn AR, Old LJ. T cell functions in granulocyte/macrophage colony-stimulating factor deficient mice. *Proc Natl Acad Sci U S A* 1997;94:12557-61.
18. Yang H, Wei J, Zhang H, Lin L, Zhang W, He S. Upregulation of Toll-like receptor (TLR) expression and release of cytokines from P815 mast cells by GM-CSF. *BMC Cell Biol* 2009;10:37.
19. Barreda DR, Hanington PC, Belosevic M. Regulation of myeloid development and function by colony stimulating factors. *Dev Comp Immunol* 2004;28:509-54.
20. Kingston D, Schmid MA, Onai N, Obata-Onai A, Baumjohann D, Manz MG. The concerted action of GM-CSF and Flt3-ligand on *in vivo* dendritic cell homeostasis. *Blood* 2009;114:835-43.
21. Mausberg AK, Jander S, Reichmann G. Intracerebral granulocyte-macrophage colony-stimulating factor induces functionally competent dendritic cells in the mouse brain. *Glia* 2009;57:1341-50.
22. Daro E, Pulendran B, Brasel K, Teepe M, Pettit D, Lynch DH, et al. Polyethylene glycol-modified GM-CSF expands CD11b(high)CD11c (high) but not CD11b(low)CD11c(high) murine dendritic cells *in vivo*: a comparative analysis with Flt3 ligand. *J Immunol* 2000;165:49-58.
23. Esashi E, Wang YH, Peng O, Qin XF, Liu YJ, Watowich SS. The signal transducer STAT5 inhibits plasmacytoid dendritic cell development by suppressing transcription factor IRF8. *Immunity* 2008;28:509-20.
24. Schlitzer A, Loschko J, Mair K, Vogelmann R, Henkel L, Einwachter H, et al. Identification of CCR9⁺ murine plasmacytoid DC precursors with plasticity to differentiate into conventional DCs. *Blood* 2011;117:6562-70.
25. Ghirelli C, Zollinger R, Soumelis V. Systematic cytokine receptor profiling reveals GM-CSF as a novel TLR-independent activator of human plasmacytoid dendritic cells. *Blood* 2010;115:5037-40.
26. Banachereau J, Palucka AK. Dendritic cells as therapeutic vaccines against cancer. *Nat Rev Immunol* 2005;5:296-306.
27. Munn DH, Sharma MD, Hou D, Baban B, Lee JR, Antonia SJ, et al. Expression of indoleamine 2,3-dioxygenase by plasmacytoid dendritic cells in tumor-draining lymph nodes. *J Clin Invest* 2004;114:280-90.
28. Labidi-Galy SI, Sisirak V, Meeus P, Gobert M, Treilleux I, Bajard A, et al. Quantitative and functional alterations of plasmacytoid dendritic cells

- contribute to immune tolerance in ovarian cancer. *Cancer Res* 2011; 71:5423–34.
29. Zou W, Machelon V, Coulomb-L'Hermin A, Borvak J, Nome F, Isaeva T, et al. Stromal-derived factor-1 in human tumors recruits and alters the function of plasmacytoid precursor dendritic cells. *Nat Med* 2001;7: 1339–46.
 30. Kim R, Emi M, Tanabe K, Arihiro K. Potential functional role of plasmacytoid dendritic cells in cancer immunity. *Immunology* 2007;121: 149–57.
 31. Villadangos JA, Young L. Antigen-presentation properties of plasmacytoid dendritic cells. *Immunity* 2008;29:352–61.
 32. Sapozhnikov A, Fischer JA, Zaft T, Krauthgamer R, Dzionek A, Jung S. Organ-dependent *in vivo* priming of naive CD4⁺, but not CD8⁺, T cells by plasmacytoid dendritic cells. *J Exp Med* 2007;204:1923–33.
 33. Di Pucchio T, Chatterjee B, Smed-Sorensen A, Clayton S, Palazzo A, Montes M, et al. Direct proteasome-independent cross-presentation of viral antigen by plasmacytoid dendritic cells on major histocompatibility complex class I. *Nat Immunol* 2008;9:551–7.
 34. Palamara F, Meindl S, Holcmann M, Luhrs P, Stingl G, Sibilio M. Identification and characterization of pDC-like cells in normal mouse skin and melanomas treated with imiquimod. *J Immunol* 2004;173: 3051–61.
 35. Molenkamp BG, Sluijter BJ, van Leeuwen PA, Santegoets SJ, Meijer S, Wijnands PG, et al. Local administration of PF-3512676 CpG-B instigates tumor-specific CD8⁺ T-cell reactivity in melanoma patients. *Clin Cancer Res* 2008;14:4532–42.
 36. Aspord C, Charles J, Leccia MT, Laurin D, Richard MJ, Chaperot L, et al. A novel cancer vaccine strategy based on HLA-A*0201 matched allogeneic plasmacytoid dendritic cells. *PLoS ONE* 2010; 5:e10458.
 37. Drobits B, Holcmann M, Amberg N, Swiecki M, Grundtner R, Hammer M, et al. Imiquimod clears tumors in mice independent of adaptive immunity by converting pDCs into tumor-killing effector cells. *J Clin Invest* 2012;122:575–85.
 38. Fonteneau JF, Gilliet M, Larsson M, Dasilva I, Munz C, Liu YJ, et al. Activation of influenza virus-specific CD4⁺ and CD8⁺ T cells: a new role for plasmacytoid dendritic cells in adaptive immunity. *Blood* 2003; 101:3520–6.
 39. Le Bon A, Etchart N, Rossmann C, Ashton M, Hou S, Gewert D, et al. Cross-priming of CD8⁺ T cells stimulated by virus-induced type I interferon. *Nat Immunol* 2003;4:1009–15.
 40. Honda K, Sakaguchi S, Nakajima C, Watanabe A, Yanai H, Matsumoto M, et al. Selective contribution of IFN-alpha/beta signaling to the maturation of dendritic cells induced by double-stranded RNA or viral infection. *Proc Natl Acad Sci U S A* 2003;100:10872–7.
 41. Blasius AL, Cella M, Maldonado J, Takai T, Colonna M. Siglec-H is an IPC-specific receptor that modulates type I IFN secretion through DAP12. *Blood* 2006;107:2474–6.
 42. Dang Y, Wagner WM, Gad E, Rastetter L, Berger CM, Holt GE, et al. Dendritic cell-activating vaccine adjuvants differ in the ability to elicit antitumor immunity due to an adjuvant-specific induction of immunosuppressive cells. *Clin Cancer Res* 2012;18:3122–31.

Cancer Immunology Research

TLR7 Ligand Augments GM-CSF–Initiated Antitumor Immunity through Activation of Plasmacytoid Dendritic Cells

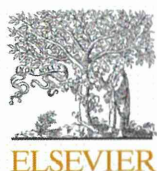
Megumi Narusawa, Hiroyuki Inoue, Chika Sakamoto, et al.

Cancer Immunol Res 2014;2:568-580. Published OnlineFirst April 10, 2014.

Updated version	Access the most recent version of this article at: doi:10.1158/2326-6066.CIR-13-0143
Supplementary Material	Access the most recent supplemental material at: http://cancerimmunolres.aacrjournals.org/content/suppl/2014/04/17/2326-6066.CIR-13-0143.DC1.html

Cited Articles	This article cites by 42 articles, 17 of which you can access for free at: http://cancerimmunolres.aacrjournals.org/content/2/6/568.full.html#ref-list-1
-----------------------	---

E-mail alerts	Sign up to receive free email-alerts related to this article or journal.
Reprints and Subscriptions	To order reprints of this article or to subscribe to the journal, contact the AACR Publications Department at pubs@aacr.org .
Permissions	To request permission to re-use all or part of this article, contact the AACR Publications Department at permissions@aacr.org .



Analysis of essential pathways for self-renewal in common marmoset embryonic stem cells

Takenobu Nii^{a,1}, Tomotoshi Marumoto^{a,b,1}, Hiroataka Kawano^a, Saori Yamaguchi^a, Jiyuan Liao^a, Michiyo Okada^a, Erika Sasaki^{c,d}, Yoshie Miura^a, Kenzaburo Tani^{a,b,*}

^aDivision of Molecular and Clinical Genetics, Medical Institute of Bioregulation, Kyushu University, 3-1-1, Maidashi, Higashi-ku, Fukuoka 812-8582, Japan

^bDepartment of Advanced Molecular and Cell Therapy, Kyushu University Hospital, 3-1-1, Maidashi, Higashi-ku, Fukuoka 812-8582, Japan

^cCentral Institute for Experimental Animals, Kawasaki, Kanagawa 216-0001, Japan

^dKeio Advanced Research Center, Keio University School of Medicine, Tokyo 160-8582, Japan

ARTICLE INFO

Article history:

Received 21 November 2013

Revised 12 February 2014

Accepted 12 February 2014

Keywords:

Embryonic stem cells

Common marmoset

bFGF

TGFβ

Self-renewal

ABSTRACT

Common marmoset (CM) is widely recognized as a useful non-human primate for disease modeling and preclinical studies. Thus, embryonic stem cells (ESCs) derived from CM have potential as an appropriate cell source to test human regenerative medicine using human ESCs. CM ESCs have been established by us and other groups, and can be cultured *in vitro*. However, the growth factors and downstream pathways for self-renewal of CM ESCs are largely unknown. In this study, we found that basic fibroblast growth factor (bFGF) rather than leukemia inhibitory factor (LIF) promoted CM ESC self-renewal via the activation of phosphatidylinositol-3-kinase (PI3K)-protein kinase B (AKT) pathway on mouse embryonic fibroblast (MEF) feeders. Moreover, bFGF and transforming growth factor β (TGFβ) signaling pathways cooperatively maintained the undifferentiated state of CM ESCs under feeder-free condition. Our findings may improve the culture techniques of CM ESCs and facilitate their use as a preclinical experimental resource for human regenerative medicine.

© 2014 The Authors. Published by Elsevier B.V. on behalf of the Federation of European Biochemical Societies. This is an open access article under the CC BY-NC-ND license (<http://creativecommons.org/licenses/by-nc-nd/3.0/>).

1. Introduction

Human regenerative medicine, including transplantation of various functional cells differentiated from embryonic stem cells (ESCs) or induced pluripotent stem cells (iPSCs), is considered to have great potential for treating various incurable diseases, and has thus attracted much public attention. However, preclinical studies using animal disease models are required to evaluate the efficacy and safety of ESC/iPSC-derived cells prior to their clinical

application. Common marmoset (CM, *Callithrix jacchus*) has recently been recognized as a useful non-human primate for such studies, because of its small size, high reproductive capacity, and genetic similarity to humans [1].

Understanding the molecular mechanisms governing the self-renewal of ESCs is important for the development of technologies to differentiate them into functional cells. Although both human and mouse ESCs are able to self-renew on feeder cells *in vitro*, their growth factor requirements for self-renewal are different. Basic fibroblast growth factor (bFGF), which activates phosphatidylinositol-3-kinase (PI3K)-protein kinase B (AKT) [2,3] and mitogen-activated protein/extracellular signal-regulated kinase kinase (MEK)-extracellular signal-regulated kinase (ERK) pathways [2–8], and transforming growth factor β (TGFβ) leading to the activation of mothers against decapentaplegic homolog 2/3 (SMAD2/3) [2,6–11], maintain the self-renewal of human ESCs and mouse epiblast stem cells (EpiSCs). Conversely, in mouse ESCs, leukemia inhibitory factor (LIF), which activates janus kinase (JAK)-signal transducer and activator of transcription 3 (STAT3) and PI3K-AKT pathways, is known to play important roles in maintaining self-renewal [12–14].

Abbreviations: AKT, protein kinase B; bFGF, basic fibroblast growth factor; CM, common marmoset; EB, embryoid body; EpiSCs, epiblast stem cells; ERK, extracellular signal-regulated kinase; ESCs, embryonic stem cells; FCM, flow cytometry; iPSCs, induced pluripotent stem cells; JAK, janus kinase; KSR, knockout serum replacement; LIF, leukemia inhibitory factor; MEFs, mouse embryonic fibroblasts; MEK, mitogen-activated protein/extracellular signal-regulated kinase kinase; PI3K, phosphatidylinositol-3-kinase; RT-PCR, reverse transcription-polymerase chain reaction; SMAD2/3, mothers against decapentaplegic homolog 2/3; STAT3, signal transducer and activator of transcription 3; TGFβ, transforming growth factor β

* Corresponding author at: Division of Molecular and Clinical Genetics, Medical Institute of Bioregulation, Kyushu University, 3-1-1, Maidashi, Higashi-ku, Fukuoka 812-8582, Japan. Tel.: +81 92 642 6434; fax: +81 92 642 6444.

E-mail address: taniken@bioreg.kyushu-u.ac.jp (K. Tani).

¹ The first two authors contributed equally to this work.

<http://dx.doi.org/10.1016/j.fob.2014.02.007>

2211-5463/© 2014 The Authors. Published by Elsevier B.V. on behalf of the Federation of European Biochemical Societies. This is an open access article under the CC BY-NC-ND license (<http://creativecommons.org/licenses/by-nc-nd/3.0/>).